16. C. J. Marshall, *Cell* **80**, 179 (1995).
17. S. Sasagawa, Y. Ozaki, K. Fujita, S. Kuroda, *Nat. Cell Biol.* **7**, 365 (2005).
18. L. O. Murphy, J. Blenis, *Trends Biochem. Sci.* **31**, 268 (2006).
19. M. Villedieu *et al.*, *Gynecol. Oncol.* **101**, 507 (2006).
20. B. K. Choi, C. H. Choi, H. L. Oh, Y. K. Kim, *Neurotoxicity* **25**, 915 (2004).
21. S. D. Santos, P. J. Verveer, P. I. Bastiaens, *Nat. Cell Biol.* **9**, 247 (2007).
22. A. Acharya, S. B. Ruvinov, J. Gal, C. Vinson, *Biochemistry* **41**, 14122 (2002).
23. M. Ramezani-Rad, *Curr. Genet.* **43**, 161 (2003).
24. C. Wu, E. Leberer, D. Y. Thomas, M. Whiteway, *Mol. Biol. Cell* **10**, 2425 (1999).
25. X. L. Zhan, R. J. Deschenes, K. L. Guan, *Genes Dev.* **11**, 1690 (1997).
26. J. Andersson, D. M. Simpson, M. Qi, Y. Wang, E. A. Elion, *EMBO J.* **23**, 2564 (2004).
27. R. P. Bhattacharyya *et al.*, *Science* **311**, 822 (2006).
28. N. T. Ingolia, A. W. Murray, *Curr. Biol.* **17**, 668 (2007).
29. N. Barkai, S. Leibler, *Nature* **387**, 913 (1997).
30. B. Alberts *et al.*, *Essential Cell Biology* (Garland Science, London, ed. 2, 2003)
31. N. Rosenfeld, M. B. Elowtiz, U. Alon, *J. Mol. Biol.* **323**, 785 (2002).
32. M. Ptashne, A. Gann, *Genes and Signals* (Cold Spring Harbor Laboratory Press, Cold Spring Harbor, NY, 2001)
33. D. C. Popescu, A. J. Ham, B. H. Shieh, *J. Neurosci.* **26**, 8570 (2006).
34. K. Scott, C. S. Zuker, *Nature* **395**, 805 (1998).
35. F. D. Smith, L. K. Langeberg, J. D. Scott, *Trends Biochem. Sci.* **31**, 316 (2006).
36. S. C. Strickfaden *et al.*, *Cell* **128**, 519 (2007).
37. P. Mishra *et al.*, *Cell* **131**, 80 (2007).
38. We thank H. El-Samad, T. Kortemme, H. Madhani, C. Tang, C. Voigt, J. Weissman, and the Lim laboratory for advice and comments. Supported by University of California GREAT fellowship (C.J.B.), American Cancer Society Postdoctoral Fellowship (N.C.H.), Jane Coffin Childs Fellowship (S.Y.) and grants from the U.S. Defense Advanced Research Projects Agency (Biological Input/Output Systems); NIH Nanomedicine Development Centers (Roadmap); National Institute of General Medical Science, NIH; Packard Foundation; and Rogers Family Foundation (W.A.L.).

Supporting Online Material

www.sciencemag.org/cgi/content/full/319/5869/1539/DC1
Materials and Methods
SOM Text
Figs. S1 to S6
Tables S1 to S3
References

1 October 2007; accepted 11 February 2008
10.1126/science.1151153

Synaptic Theory of Working Memory

Gianluigi Mongillo,[1]*† Omri Barak,[2]* Misha Tsodyks[2]‡§

It is usually assumed that enhanced spiking activity in the form of persistent reverberation for several seconds is the neural correlate of working memory. Here, we propose that working memory is sustained by calcium-mediated synaptic facilitation in the recurrent connections of neocortical networks. In this account, the presynaptic residual calcium is used as a buffer that is loaded, refreshed, and read out by spiking activity. Because of the long time constants of calcium kinetics, the refresh rate can be low, resulting in a mechanism that is metabolically efficient and robust. The duration and stability of working memory can be regulated by modulating the spontaneous activity in the network.

Working memory (WM) enables the temporary holding of information for processing purposes, playing a crucial role in the execution of a wide range of cognitive tasks (*1*). In the delayed-response paradigm, a stimulus that is briefly presented to an animal has to be kept for several seconds until the execution of a task. Enhanced, stimulus-specific spiking activity has been observed during this delay period and is considered to be a neuronal correlate of WM (*2*–*5*). The current theoretical framework holds that delay activity emerges either from intrinsic cell properties (*6*, *7*) or as persistent reverberations in selective neural populations coding for different memories (*8*–*12*). These populations are formed during learning via long-term synaptic modifications (*13*). However, electrophysiological studies have shown that the delay activity increase can be very modest (*14*, *15*), sometimes disappearing completely during part of the delay period (*16*). These observations suggest that WM might not reside entirely in the spiking activity. Furthermore, holding information in a spiking form is energetically expensive because of the high metabolic cost of action potentials (*17*). Here, we present an alternative account based on properties of excitatory synaptic transmission in the prefrontal cortex (PFC) (*18*). The PFC is a cortical area implicated in WM (*4*), and excitatory synaptic transmission in this area can be markedly facilitatory, unlike sensory areas where it is mostly depressing (*19*, *20*). We therefore propose that an item is maintained in the WM state by short-term synaptic facilitation mediated by increased residual calcium levels at the presynaptic terminals of the neurons that code for this item (*21*). Because removal of residual calcium from presynaptic terminals is a relatively slow process (*22*, *23*), the memory can be transiently held for about 1 s without enhanced spiking activity.

We implemented this mechanism with a recurrent network of integrate-and-fire neurons (*24*). The network encodes a set of memories (items) by randomly composed selective populations of excitatory neurons (Fig. 1B). Connections between the neurons coding for the same memory are stronger than connections between different populations, mimicking the result of prior long-term Hebbian learning (*25*) or intrinsic clustering of recurrent connections (*26*). Inhibitory neurons are connected to the excitatory ones in a nonstructured way, resulting in competition between different memories [see supporting online material (SOM)]. All excitatory-to-excitatory connections display facilitating transmission, described by a phenomenological model of short-term plasticity (*20*, *27*). Synaptic efficacy is modulated by the amount of available resources (x, normalized so that $0 < x < 1$) and the utilization parameter (u) that defines the fraction of resources used by each spike, reflecting the residual calcium level (*22*, *23*) (Fig. 1A and SOM). Upon a spike, an amount ux of the available resources is used to produce the postsynaptic current, thus reducing x. This process mimics neurotransmitter depletion. The spike also increases u, mimicking calcium influx into the presynaptic terminal and its effects on release probability. Between spikes, x and u recover to their baseline levels ($x = 1$ and $u = U$) with time constants τ_D (depressing) and τ_F (facilitating), respectively. The phenomenological model reproduces the behavior of cortical synapses, both depressing ($\tau_D > \tau_F$) and facilitating ($\tau_F > \tau_D$) (*27*). For PFC facilitating excitatory connections, the experimental fit reports $\tau_F >> \tau_D$ (*18*), with τ_F on the order of 1 s.

The simulations begin with loading one item into WM by providing transient external excitation to the corresponding neural population (Fig. 2A). The population activity increases for the duration of the input, changing the internal state of the synaptic connections. The connections are both depressed (reduced x) and facilitated (increased u), with depression dominant on the time scale of τ_D and facilitation dominant on the time scale of τ_F (where $\tau_D = 0.2$ s and $\tau_F = 1.5$ s; see SOM for all parameter values). As long as the synapses remain facilitated, the memory can be reactivated by presenting a weak nonspecific excitatory input to the whole network (gray shading), even though the neural activity is at the spontaneous level. Reactivation is expressed as a short epoch of synchronized activity ["population spike" (PS)], where almost every neuron in the population fires a spike within an interval of about 20 ms (*28*, *29*). Even though the reactivating signal is nonspecific (that is, it uniformly

[1]Group for Neural Theory, Département d'Etudes Cognitives, Ecole Normale Supérieure et Collège-de-France, Paris, France. [2]Department of Neurobiology, Weizmann Institute of Science, Rehovot, Israel.

*These authors contributed equally to this work.
†Present address: Laboratoire de Neurophysique et Physiologie, Université Paris-Descartes, CNRS-UMR8119, and Franco-Israeli Laboratory of System Neurophysiology and Neurophysics, Paris, France.
‡CNRS visiting member of the Group for Neural Theory, Ecole Normale Supérieure et Collège-de-France.
§To whom correspondence should be addressed. E-mail: misha@weizmann.ac.il

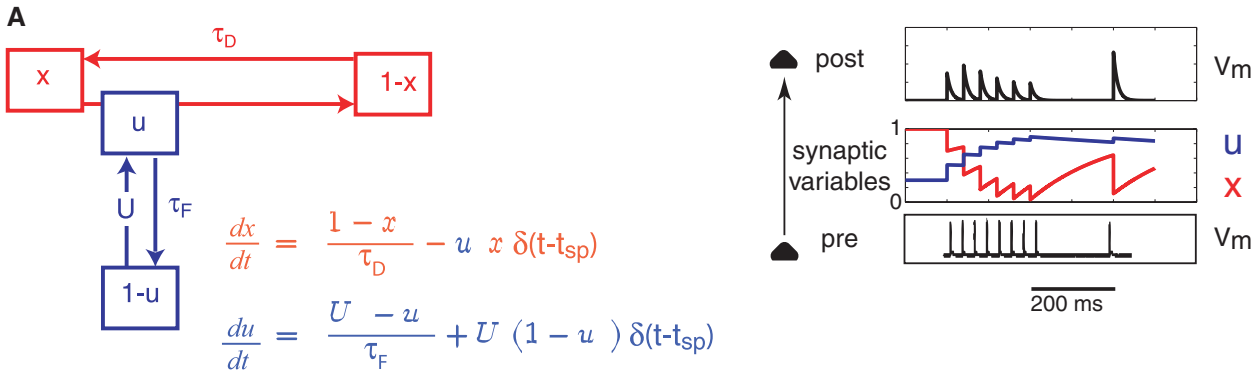

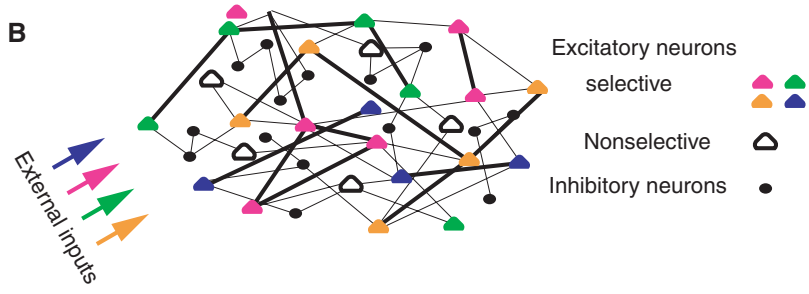

Fig. 1. Physiology and anatomy of the network. (**A**) Short-term synaptic plasticity model. (Left) Kinetic scheme with the corresponding equations for synaptic variables. δ, Dirac delta function; t_{sp}, time of presynaptic spike. (Right) Example of the postsynaptic response to a train of presynaptic action potentials in the case of a facilitating connection. During the train, *u* increases (facilitation) and *x* decreases (depression). Synaptic efficacy is modulated by the product *ux*. v_m, membrane potential. (**B**) Network architecture. Colored triangles are excitatory neurons that code for different memories. Black open triangles are nonselective excitatory neurons. Black circles are inhibitory neurons with nonstructured connections to the entire network.

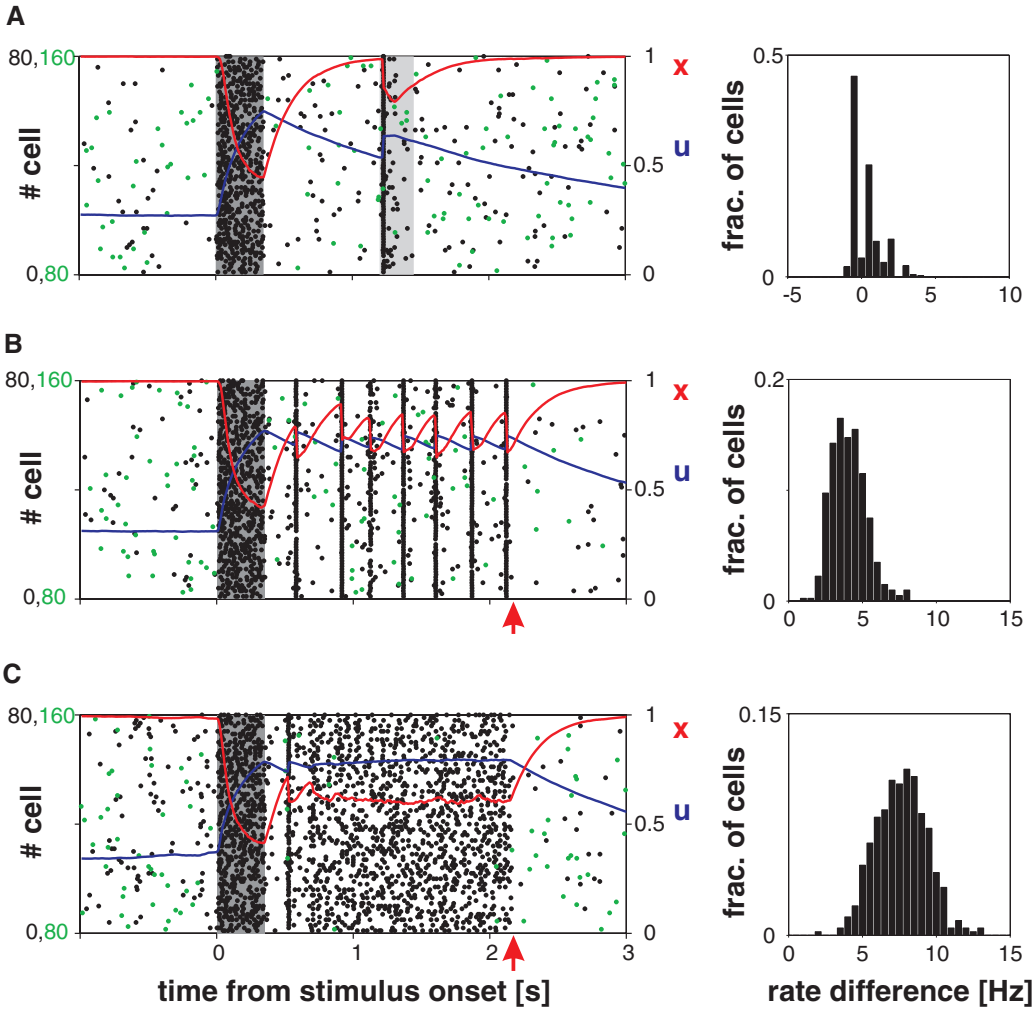

Fig. 2. Memory maintenance with synaptic facilitation. (**A**) The item is loaded into the memory by activating the corresponding population at time *t* = 0 (dark shading). A nonspecific read-out signal is applied to the entire excitatory network as explained in the text (gray shading), leading to the selective reactivation of the target population via the PS. Black and green dots, spike rasters from a subset (10%) of neurons from the targeted and one of the nontargeted populations, respectively; red curve, average value of *x* in the synaptic connections of the target population; blue curve, average value of *u* for the same synapses. (**B**) Same as (A), with an increased background input. The target population reactivates spontaneously with a set of PSs. Red arrow indicates termination of excitation. (**C**) A further increase in background input leads to WM with asynchronous elevated firing in the target population. (Right) Corresponding histograms for (A) to (C) of the difference in firing rate between the delay period and the spontaneous state for different neurons in the target population [note the different *x* axis in (A)]. The delay period is defined in (A) as the interval after the termination of the selective input until the onset of the read-out signal and in (B) and (C) as the period until the decrease of external excitation.

targets all the neurons), the network response is memory-specific: The neurons coding for the loaded item produce a PS; the others stay at baseline activity level. The PS also refreshes the memory by producing additional facilitation, thus enabling subsequent memory reactivations. In the absence of reactivating signals, the memory fades away over a time scale on the order of τ_F.

In the above scenario, the network has a single stable activity state corresponding to the spontaneous activity, thus appropriately timed external signals are required to extract the memory from synaptic to spiking form. A more persistent form of WM requires the selective population to exhibit a bistable activity regime, where the spontaneous state coexists with another stable state (*8*). Our network can be forced into this regime by increasing spontaneous activity by means of a global nonspecific background input (see SOM for the mathematical analysis). Accordingly, we simulated the network for increasing levels of background input. In the bistable regime, PSs become persistent without reactivating inputs (Fig. 2B). Each reactivation increases u and decreases x, the latter terminating the PS. The time between subsequent PSs is controlled by the recovery from synaptic depression so that the PSs tend to occur with a period on the order of τ_D. With a τ_D compatible with (*18*), this would correspond to cortical oscillations in the theta-range, as observed during WM experiments (*30*, *31*). Because $\tau_F >> \tau_D$, the decay of the utilization factor is balanced by the increase produced by the PSs, so that u remains at sufficiently high levels for subsequent PSs to emerge. Persistent PSs can be terminated by reducing background input, thus restoring the network to the transient regime. A different model of persistent PSs is based on the increase in asynchronous transmitter release (*32*). In the simulation presented in Fig. 2B, neurons coding for a given memory exhibit highly coherent firing during the PSs. In more realistic networks, PSs could be broader and consist of random subpopulations of neurons, resulting in less pronounced synchrony (fig. S2). If nonspecific background input increases further, the network exhibits bistability between a spontaneous state and an asynchronous state of enhanced firing rate (Fig. 2C). Information about the memory is maintained in both synaptic and spiking form. This regime exists for sufficiently strong recurrent connections, which could possibly result from extensive learning.

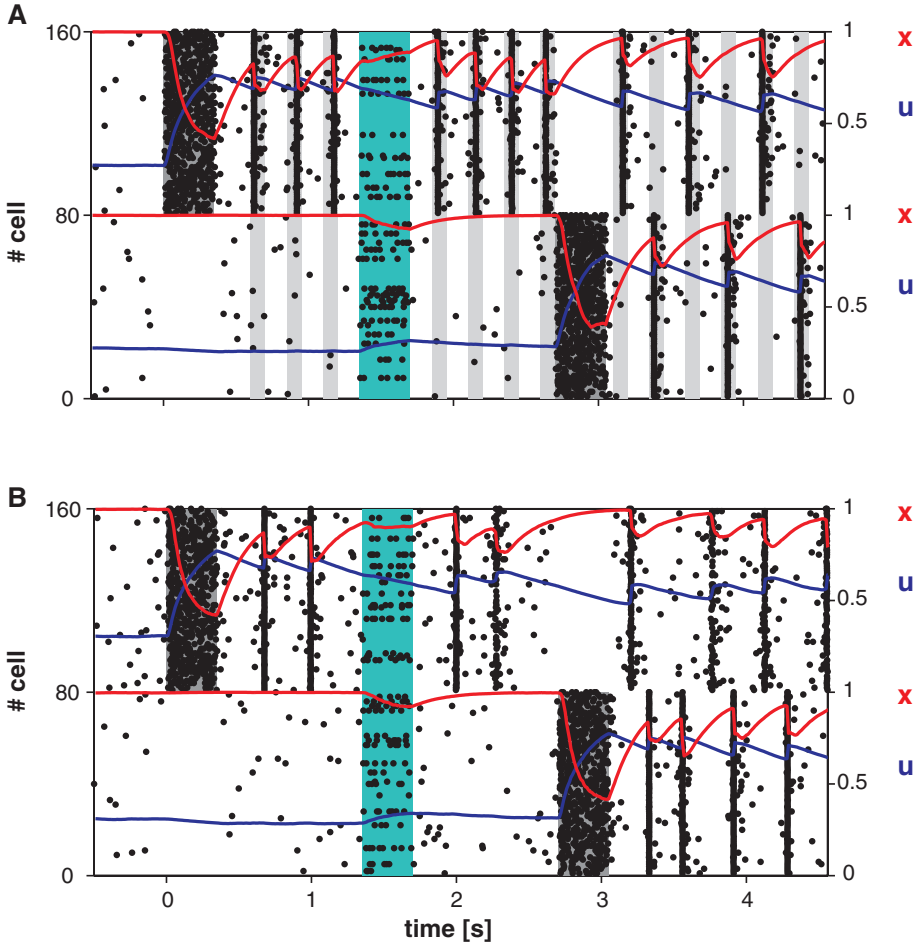

Fig. 3. Robustness to noise and two-item memory. The first item is loaded into memory at $t = 0$ (dark shading). The second item is loaded into memory at $t = 2.7$ s. Teal shading indicates a random nonspecific input to 15% of the excitatory neurons. (**A**) Periodic sequence of nonspecific external inputs is used to refresh the memory (gray shading). (**B**) Persistent PSs. Dots, rasters of 10% of the first (0 to 79) and second (80 to 159) populations' neurons; red and blue curves, same as in Fig. 2.

The use of residual calcium at synaptic terminals as a memory "buffer" requires low emission rates (Fig. 2, histograms). Moreover, the buffer content is not substantially affected by the neural activity in the rest of the cortex. When we presented the network with a noisy input that targeted a random subset of excitatory neurons for a brief duration, the increased firing of neurons receiving the input suppressed the memory-related spiking activity (Fig. 3, teal shading). The information, however, remained in the increased utilization factor in the memory population; hence, the spiking activity resumed after the termination of the suppressing input. The same feature enables the network to keep multiple items simultaneously with interleaved PSs (*33*). We illustrated this possibility in two different conditions: (i) when the network has a single activity state and PSs result from a sequence of reactivating signals (Fig. 3A) or (ii) when the network exhibits persistent PSs (Fig. 3B). When a new item is presented, the previous memory is temporarily suppressed (dark shading), after which the network maintains both memories by subsequent reactivations of the two populations. When the network is in the regime of externally generated PSs, two-item WM results in the same oscillation frequency in the global activity as that of the one-item memory (*30*), whereas in the regime of persistent PSs, two-item memory results in higher global frequency. In more realistic implementations of the model, an increase in frequency may be less pronounced also in the persistent regime (fig. S2).

Consequently, we propose that WM can be maintained by short-term synaptic facilitation. Accumulation of residual calcium in the presynaptic terminals could carry the information about the recalled memory in a working form, reducing the need for metabolically costly action potentials. The memories are transformed into spiking activity, either as a result of global reactivating input to the network or by virtue of the intrinsic network dynamics. Not all encountered stimuli enter WM, and we thus expect the basal modality of the network to be the transient one. The decision to allow items into WM is mediated by attention, which we suggest is represented by the global excitatory input, either in tonic or oscillating mode. The performance of human observers on memory tasks is positively correlated with the level of neural activity during the presentation of the items (*34*).

The model predicts that residual calcium at the presynaptic terminals should be tonically enhanced during WM, even when there is no noticeable increase in the firing rate. This prediction is in contrast to the model of (*7*) where WM is mediated by propagating calcium wave-

fronts along dendritic processes. Suppressing the spiking activity for a period of several hundred milliseconds (*35*) should still allow for the memory to reactivate after the suppressing input is withdrawn. We also expect that groups of neurons could exhibit brief epochs of coherent firing. The model provides a possible target for a pharmacological interference with WM. In particular, manipulations that modify the facilitation/depression balance in the memory-related cortical areas (*36*) are predicted to have a strong effect on the stability and duration of memory.

References and Notes

1. A. D. Baddeley, G. J. Hitch, in *The Psychology of Learning and Motivation: Advances in Research and Theory*, vol. 8, G. H. Bower, Ed. (Academic Press, New York, 1974), pp. 47–89.
2. J. M. Fuster, G. E. Alexander, *Science* **173**, 652 (1971).
3. Y. Miyashita, *Nature* **335**, 817 (1988).
4. P. S. Goldman-Rakic, *Neuron* **14**, 477 (1995).
5. E. K. Miller, C. A. Erickson, R. Desimone, *J. Neurosci.* **16**, 5154 (1996).
6. E. Fransen, B. Tahvildari, A. V. Egorov, M. E. Hasselmo, A. A. Alonso, *Neuron* **49**, 735 (2006).
7. Y. Loewenstein, H. Sompolinsky, *Nat. Neurosci.* **6**, 961 (2003).
8. D. J. Amit, *Behav. Brain Sci.* **18**, 617 (1995).
9. X. J. Wang, *Trends Neurosci.* **24**, 455 (2001).
10. N. Brunel, *Cereb. Cortex* **13**, 1151 (2003).
11. M. S. Goldman *et al.*, *Cereb. Cortex* **13**, 1185 (2003).
12. C. K. Machens, R. Romo, C. D. Brody, *Science* **307**, 1121 (2005).
13. D. O. Hebb, *The Organization of Behavior* (Wiley, New York, 1949).
14. Y. Naya, K. Sakai, Y. Miyashita, *Proc. Natl. Acad. Sci. U.S.A.* **93**, 2664 (1996).
15. M. Shafi *et al.*, *Neuroscience* **146**, 1082 (2007).
16. G. Rainer, E. K. Miller, *Eur. J. Neurosci.* **15**, 1244 (2002).
17. D. Attwell, S. B. Laughlin, *J. Cereb. Blood Flow Metab.* **21**, 1133 (2001).
18. Y. Wang *et al.*, *Nat. Neurosci.* **9**, 534 (2006).
19. A. M. Thomson, *J. Physiol. (London)* **502**, 131 (1997).
20. H. Markram, Y. Wang, M. Tsodyks, *Proc. Natl. Acad. Sci. U.S.A.* **95**, 5323 (1998).
21. B. Katz, R. Miledi, *J. Physiol. (London)* **195**, 481 (1968).
22. R. S. Zucker, W. G. Regehr, *Annu. Rev. Physiol.* **64**, 355 (2002).
23. R. Bertram, A. Sherman, E. F. Stanley, *J. Neurophysiol.* **75**, 1919 (1996).
24. Materials and methods are available as supporting material on *Science* Online.
25. J. J. Hopfield, *Proc. Natl. Acad. Sci. U.S.A.* **79**, 2554 (1982).
26. S. Song, P. J. Sjöström, M. Reigl, S. Nelson, D. B. Chklovskii, *PLoS Biol.* **3**, e68 (2005).
27. M. Tsodyks, K. Pawelzik, H. Markram, *Neural Comput.* **10**, 821 (1998).
28. M. Tsodyks, A. Uziel, H. Markram, *J. Neurosci.* **20**, RC50 (2000).
29. A. Loebel, M. Tsodyks, *J. Comput. Neurosci.* **13**, 111 (2002).
30. S. Raghavachari *et al.*, *J. Neurosci.* **21**, 3175 (2001).
31. H. Lee, G. V. Simpson, N. K. Logothetis, G. Rainer, *Neuron* **45**, 147 (2005).
32. V. Volman, R. C. Gerkin, P.-M. Lau, E. Ben-Jacob, G.-Q. Bi, *Phys. Biol.* **4**, 91 (2007).
33. D. Horn, M. Usher, *Phys. Rev. A* **40**, 1036 (1989).
34. L. J. Otten, R. N. A. Henson, M. D. Rugg, *Nat. Neurosci.* **5**, 1339 (2002).
35. F. Zhang *et al.*, *Nature* **446**, 633 (2007).
36. T. Sippy, A. Cruz-Martin, A. Jeromin, F. E. Schweizer, *Nat. Neurosci.* **6**, 1031 (2003).

37. We thank B. Blumenfeld and M. Segal for helpful comments on the manuscript. G.M. is supported by BACS consortium grant FP6-IST-027140 and BIND Marie Curie Team of Excellence grant MECT-CT-2005-024831. O.B. is supported by the Azrieli Foundation and the Kahn Family Research Center for Systems Biology of the Human Cell. M.T. is supported by the Israeli Science Foundation, the Irving B. Harris Foundation, and the Abe and Kathryn Selsky Foundation.

Supporting Online Material

www.sciencemag.org/cgi/content/full/319/5869/1543/DC1
SOM Text
Figs. S1 and S2
Table S1
References

20 September 2007; accepted 21 January 2008
10.1126/science.1150769

Supporting Online Material for

Synaptic Theory of Working Memory

Gianluigi Mongillo, Omri Barak, Misha Tsodyks*

*To whom correspondence should be addressed. E-mail: misha@weizmann.ac.il

Published 14 March 2007, *Science* **319**, 1543 (2007)
DOI: 10.1126/science.1150769

This PDF file includes:

Bifurcation analysis of a single population rate model To better elucidate the dynamical mechanism of the spiking network behavior, we considered a simplified rate model consisting of a single excitatory population. The state of the population is described by the average rate E (*1*), the average utilization factor u, and the average amount of available resources x. They evolve according to (*2*):

$$\begin{aligned} \tau \frac{dE}{dt} &= -E + g(JuxE + E_0) \\ \frac{du}{dt} &= \frac{U-u}{\tau_F} + U(1-u)E \\ \frac{dx}{dt} &= \frac{1-x}{\tau_D} - uxE \end{aligned} \tag{1}$$

where $g(...)$ is the neuronal gain function, J is the strength of recurrent connections, E_0 is an external input and τ is the time constant of the rate dynamics, usually assumed to be on the order of several milliseconds. In this study, we chose the smooth gain function that has an exponentially decaying subthreshold component and a suprathreshold linear part: $g(z) = \alpha log(1 + e^{z/\alpha})$.

Because we are interested in the case of strongly facilitating connections with $\tau_F >> \tau_D$, it is instructive to consider first the fast two dimensional $E - x$ subsystem that is obtained by the first and the third of the equations 1 with a constant value of u (see (*3*) for a more detailed analysis of this system). This case corresponds to purely depressing synaptic connections. For constant inputs, the system can exhibit two possible stable behaviors: a steady state with $E = const$, and a limit cycle solution corresponding to a periodic train of population spikes that emerges when the steady state solution is unstable (see Fig. S1**A**). For given values of J and E_0, there is a certain critical value of $u = u_{cr}$ that separates these two activity regimes. In the full three-dimensional system of equations 1, there is a certain range of parameters where

these two behaviors can coexist. Intuitively, this can be understood as follows. Imagine that the network, initially in the stable steady state, is perturbed by a transient external input that evokes a single population spike. Due to facilitation, the synaptic state after the termination of the population spike is characterized by increased u (facilitation) and decreased x (depression). If, after the recovery from depression, the value of u remains above the critical value u_{cr}, the network will emit another population spike, and so on. This illustrates the bistable character of network activity (see Fig. S1**B**).

Mathematical analysis of equations 1 shows that there is a certain range of parameters where three steady-state solutions coexist (see Fig. S1**C** where these solutions are plotted *vs* the input E_0). The stability of these solutions can be analyzed by linearizing the equations 1 around the corresponding fixed points. The lower solution is stable and corresponds to the asynchronous spontaneous state of the network. When the two upper solutions first appear, they are both unstable. The uppermost solution subsequently becomes stable via a sub-critical Hopf bifurcation (see e.g. (*4*)) for higher values of the input. Before this bifurcation, a stable limit cycle appears, corresponding to the periodic train of population spikes shown on Fig. S1**B**. The range of external inputs where the limit cycle coexists with the spontaneous state corresponds to the persistent population spike regime described in the main text. The bifurcation analysis was done using XPPAUT by Bard Ermentrout.

Spiking network The network is composed of N_E excitatory and N_I inhibitory current-based integrate-and-fire neurons, whose sub-threshold depolarization dynamics is described by

$$\tau_m \dot{V}_i = -V_i + I_i^{(rec)}(t) + I_i^{(ext)}(t) \tag{2}$$

where the subscript $i = (1, \ldots, N_E + N_I)$ refers to the neuron number, τ_m is the membrane time constant, $I_i^{(rec)}(t)$ is the current mediated by recurrent synaptic connections, and $I_i^{(ext)}(t)$ is the

external current provided by distant brain areas. Membrane resistance has been absorbed into the definition of the currents in Eq. 2. Whenever the depolarization hits a fixed threshold θ (i.e. $V_i(t) \geq \theta$), the neuron emits a spike and becomes refractory for a period τ_{arp}, after which Eq. 2 resumes from a sub-threshold reset potential V_r. External currents are modeled as Gaussian white noise

$$I_i^{(ext)}(t) = \mu_{ext} + \sigma_{ext} \cdot \eta_i(t) \tag{3}$$

with $\langle \eta_i(t) \rangle = 0$, $\langle \eta_i(t) \eta_j(t') \rangle = \delta_{ij} \delta(t - t')$, so that μ_{ext} and σ_{ext}^2 are respectively the mean and the variance of the external currents. The recurrent current $I_i^{(rec)}(t)$ is the sum of the postsynaptic currents from all other neurons in the network targeting the neuron i

$$I_i^{(rec)}(t) = \sum_j \hat{J}_{ij}(t) \sum_k \delta(t - t_k^{(j)} - D_{ij}) \tag{4}$$

where $\hat{J}_{ij}(t)$ is the instantaneous efficacy (time dependence is due to short-term synaptic dynamics) of the synapse connecting neuron j to neuron i; the sum on k is over all the emission times, $t_k^{(j)}$, of presynaptic neuron j; D_{ij} is the transmission delay uniformly distributed between 1 and 5 ms. For simplicity, we neglect rise and decay times of the postsynaptic currents (see e.g. (*5*))

Excitatory-to-excitatory synapses display short-term plasticity according to (*6, 7*)

$$\dot{u}_j(t) = \frac{U - u_j(t)}{\tau_F} + U \left[1 - u_j(t)\right] \sum_k \delta(t - t_k^{(j)}) \tag{5}$$

$$\dot{x}_j(t) = \frac{1 - x_j(t)}{\tau_D} - u_j(t) x_j(t) \sum_k \delta(t - t_k^{(j)}) \tag{6}$$

where the functions multiplying the spike train are evaluated immediately before the delta functions, i.e. at $t_k^{(j)^-}$. The $\hat{J}_{ij}(t)$ to be used in Eq. 4 is given by

$$\hat{J}_{ij}(t) = J_{ij} \cdot u_j(t - D_{ij}) \cdot x_j(t - D_{ij}) \tag{7}$$

where J_{ij} is the absolute synaptic efficacy. The remaining synaptic populations, inhibitory and excitatory-to-inhibitory, exhibit linear synaptic transmission, i.e., $\hat{J}_{ij}(t) \equiv J_{ij}$. The dynamics of the network is completely described by the coupled system of non-linear equations Eqs 2-6 combined with the conditions for spike emission and refractoriness described above. These equations are integrated using an Euler scheme. Parameters used in the numerical simulations are reported in Table 1.

Long-term synaptic structuring There are p items to be memorized, each of them encoded by a subset of excitatory cells (selective population). Every selective population is formed by randomly selected fN_E neurons, where f is the coding level, enforcing the constraint that a given neuron belongs to at most one selective population (non-overlapping memories). Network connectivity is generated in the following way. Each cell receives $c(N_E + N_I)$ presynaptic connections, where c is the connectivity level, partitioned as follows: cfN_E randomly selected connections from each of the selective populations, $c(1 - fp)N_E$ randomly selected connections from the non-selective excitatory population, and cN_I randomly selected connections from the inhibitory population. The values of the efficacy for the various synaptic populations are reported in Table 1. Excitatory-to-excitatory synapses can take on two possible absolute efficacies: baseline, J_b, and potentiated, $J_p(> J_b)$. Synapses connecting two neurons within the same selective population have potentiated efficacy; Synapses connecting a selective neuron to a neuron from another selective population or to a non-selective neuron, have baseline efficacy; The remaining synapses (i.e. non-selective to selective and non-selective to non-selective) have potentiated efficacy with probability 0.1.

Overlapping populations All the figures in the main text were simulated with networks of non overlapping memories with fixed number of connections per neuron, in order to minimize the finite size effects and speed up the parameters search. We also performed more realistic simulations with overlapping memories chosen randomly with the same average size and random connectivity (*5, 8*). The qualitative behavior of the network is similar, but the population spikes are less synchronized and do not involve all the neurons in the corresponding population (Fig. S2**A**). The range of J_p for which working memory state coexists with the spontaneous activity state depends on background input and, in the case of Fig. S2, it is approximately between 0.42mV and 0.45mV. This range is about 3 times narrower than the corresponding range for the network with non-overlapping populations.

Cross-correlograms In order to examine the sharpness of population spikes, we computed cross-correlograms (CCs) for high- and low- firing neuron pairs (Fig. S2**B,C**). Spike trains are binned with a 2ms bin, corresponding to the absolute refractory period, so that in each bin there is either a spike or none. Positive and negative part of the CC are computed according to

$$CC_{+}^{(ij)}(\tau) = \frac{1}{\langle S_i \rangle \langle S_j \rangle (T-\tau)} \sum_{t=0}^{T-\tau} S_i(t) S_j(t+\tau) \quad (8)$$

$$CC_{-}^{(ij)}(\tau) = \frac{1}{\langle S_i \rangle \langle S_j \rangle (T-\tau)} \sum_{t=0}^{T-\tau} S_i(t+\tau) S_j(t) \quad (9)$$

where $S_{i(j)}(t)$ is the binned spike train of neuron $i(j)$, and $\langle S_{i(j)} \rangle$ is the corresponding average; T is the total trial duration; τ is the time-lag. Note that time is measured in units of the time bin, and CCs are normalized to 1, that would result from uncorrelated spike trains. Population-averaged CCs are then obtained by averaging the normalized single-pair CCs over all possible pairs (i, j) with $i > j$.

References and Notes

1. H. R. Wilson, J. D. Cowan, *Biophys. Journal* **12**, 1 (1972).

2. O. Barak, M. Tsodyks, *PLoS Comput Biol* **3**, e35 (2007).

3. M. Tsodyks, *Methods and models in neurophysics*, C. C. Chow, B. Gutkin, D. Hansel, C. Meunier, J. Dalibard, eds. (Elsevier, 2005), pp. 245–266.

4. Y. A. Kuznetsov, *Elements Of Applied Bifurcation Theory* (Springer, 2004).

5. S. Romani, D. J. Amit, G. Mongillo, *J. Comp. Neurosci.* **20**, 201 (2006).

6. M. Tsodyks, H. Markram, *PNAS* **94**, 719 (1997).

7. M. Tsodyks, K. Pawelzik, H. Markram, *Neural Comput.* **10**, 821 (1998).

8. E. Curti, G. Mongillo, G. La Camera, D. J. Amit, *Neural Computation* **16**, 2597 (2004).

Single-cell parameters	**E**	**I**
Θ - Spike emission threshold	20mV	20mV
$V^{(r)}$ - Reset potential	16mV	13mV
τ - Membrane time constant	15ms	10ms
$\tau^{(arp)}$ - Absolute refractory period	2ms	2ms
Network parameters	**Values**	
f - Coding level	0.10	
p - Number of memories	5	
c - Probability of synaptic contact	0.20	
N - Number of excitatory/inhibitory cells	8000	2000
$\mu^{(ext)}$ - Mean external current	23.10mV	21.0mV
$\sigma^{(ext)}$ - Standard deviation of external current	1.0mV	1.0mV
Synaptic parameters	**Values**	
J_{IE} - Synaptic efficacy $E \to I$	0.135mV	
J_{EI} - Synaptic efficacy $I \to E$	0.25mV	
J_{II} - Synaptic efficacy $I \to I$	0.20mV	
J_b - Baseline level of $E \to E$ synapses	0.10mV	
J_p - Potentiated level of $E \to E$ synapses	0.45mV	
γ_0 - Fraction of potentiated synapses before learning	0.10	
δ - Synaptic delays	$0.1 - 1$ms	
Short-term synaptic dynamics parameters	**Values**	
U - Baseline utilization factor	0.20	
τ_F - Recovery time of utilization factor	1500ms	
τ_D - Recovery time of synaptic resources	200ms	
Selective stimulation	**Values**	
T_{cue} - Duration	350ms	
A_{cue} - Contrast factor	1.15	
Reactivating signal	**Values**	
Duration	250ms	
Contrast factor	1.05	
Periodic reactivating signal	**Values**	
Duration	100ms	
Period	250	
Contrast factor	1.075	

Table S 1: Parameters used to produce Fig. 2**A** and 3**A**. For Fig. 2**B** and 3**B**, $\mu_{ext} = 23.80$mV to E neurons; For Fig. 2**C**, $\mu_{ext} = 24.30$mV to E neurons. For Fig. S2 $\mu_{ext} = 24.20$mV to E neurons, and $J_p = 0.44$mV.

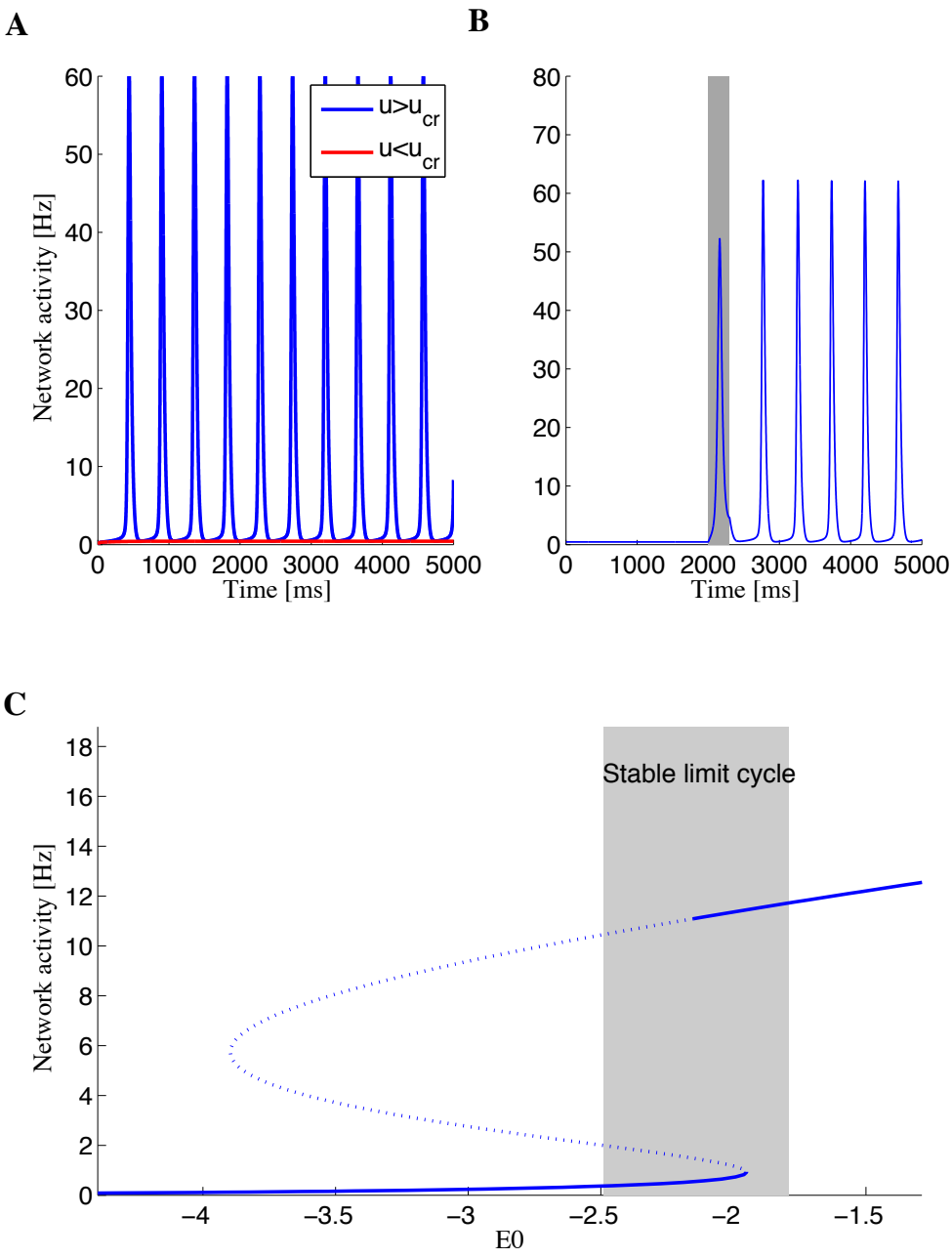

Fig. S 1: Analysis of rate model. **A** Behavior of a network with depressing synapses. Stable steady state for $u < u_{cr}$ and population spikes for $u > u_{cr}$. **B** Example of bistability with facilitating synapses. The input is fixed at $E_0 = -2.3$ except for 300 msec marked in dark shading where $E_0 = -1$. **C** Bifurcation diagram showing E as a function of E_0. Solid and dashed lines mark stable and unstable steady states respectively. The shaded area denotes the range of external input with a stable limit cycle solution. The parameters are: $J = 4$, $E_0 = -2.3$, $\alpha = 1.5$, $\tau = 13msec$, $\tau_D = 200msec$, $\tau_F = 1500msec$, $U = 0.3$. For panel A $\tau_F = 0$ resulting in $u_{cr} = 0.62$, and $u = 0.4, 0.8$ for the red and blue curves respectively.

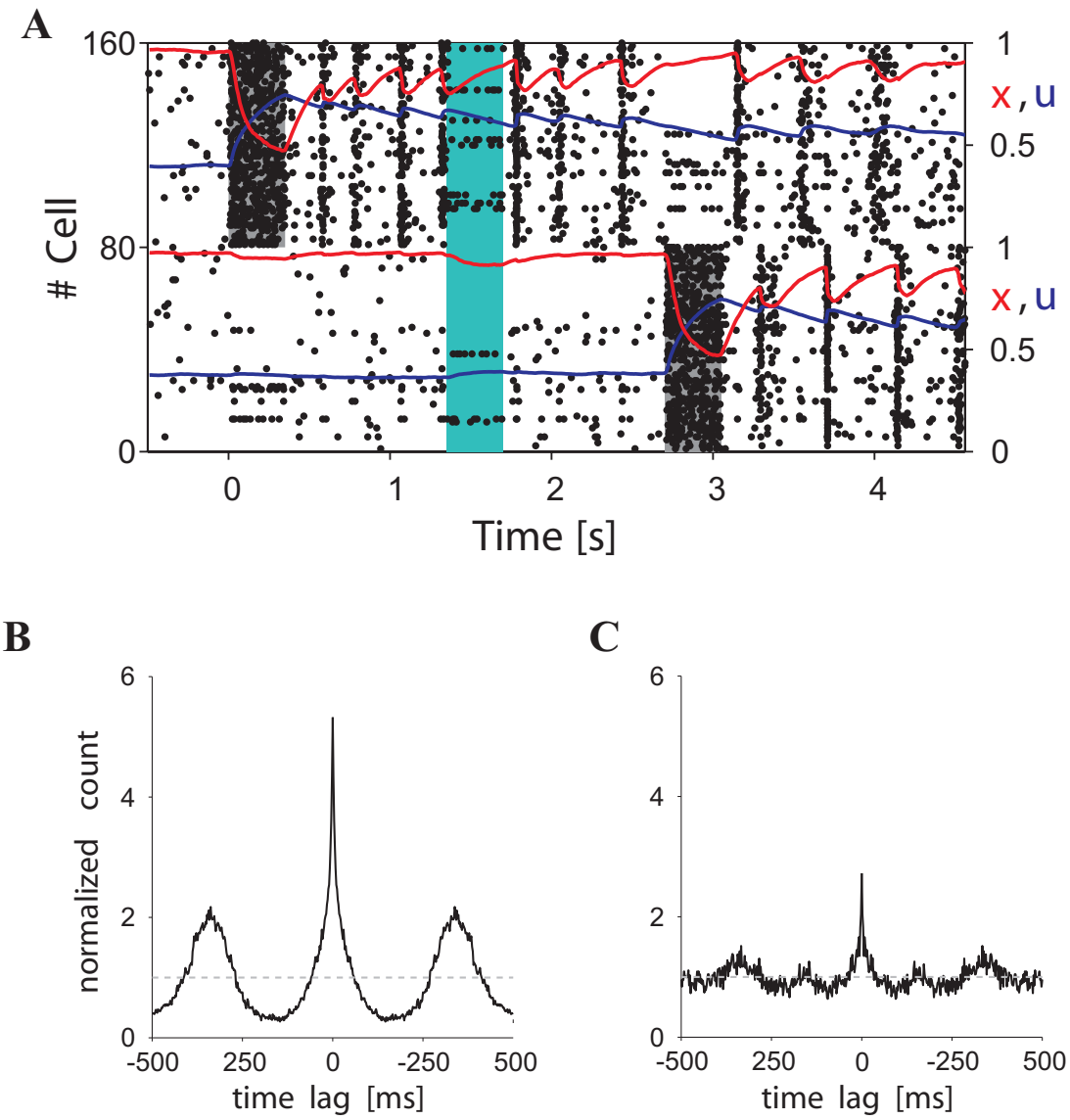

Fig. S 2: Simulation with overlapping populations. **A** The first item is loaded into memory at time zero (dark shading at the top) resulting in a train of population spikes. A non-specific noisy input is applied to randomly selected 15% of neurons in the entire excitatory network (light shading). The second item is loaded into memory at time $t = 2.7s$. Red curve - average value of available resources (x) in the synaptic connections of the target populations. Blue curve - average value of utilization factor (u) for the same synapses. **B** Averaged cross-correlogram over the population of target cells with emission rate below 5Hz during the persistent PSs regime. **C** Averaged cross-correlogram over the population of target cells with emission rate above 8Hz during the persistent PSs regime. Note that the peak at zero-lag significantly decreases, while the secondary peaks at about the period of the PSs nearly disappears. Cross-correlograms have been computed collecting data from a simulation with 50s delay period. Parameters as in Table 1 except $\mu_{ext} = 24.20$mV to E neurons and $J_p = 0.44$mV.